Attenuating the Endoplasmic Reticulum Stress Response Improves Functional Recovery After Spinal Cord Injury

SUJATA SARASWAT OHRI[1,2], **MELISSA A. MADDIE**[1,2], **YONGMEI ZHAO**[1,2], **MENGSHENG S. QIU**[1,4], **MICHAL HETMAN**[1,2,3], and **SCOTT R. WHITTEMORE**[1,2,4,*]

[1]Kentucky Spinal Cord Injury Research Center, University of Louisville, School of Medicine, MDR 616, Louisville, Kentucky

[2]Department of Neurological Surgery, University of Louisville, School of Medicine, MDR 616, Louisville, Kentucky

[3]Department of Pharmacology and Toxicology, University of Louisville, School of Medicine, MDR 616, Louisville, Kentucky

[4]Anatomical Sciences and Neurobiology, University of Louisville, School of Medicine, MDR 616, Louisville, Kentucky

Abstract

Activation of the unfolded protein response (UPR) is involved in the pathogenesis of numerous CNS myelin abnormalities; yet, its direct role in traumatic spinal cord injury (SCI)-induced demyelination is not known. The UPR is an evolutionarily conserved cell defense mechanism initiated to restore endoplasmic reticulum homeostasis in response to various cellular stresses including infection, trauma, and oxidative damage. However, if uncompensated, the UPR triggers apoptotic cell death. We demonstrate that the three signaling branches of UPR including the PERK, ATF6, and IRE1α are rapidly initiated in a mouse model of contusive SCI specifically at the injury epicenter. Immunohistochemical analyses of the various UPR markers revealed that in neurons, the UPR appeared at 6 and 24-h post-SCI. In contrast, in oligodendrocytes and astroglia, UPR persisted at least for up to 3 days post-SCI. The UPR-associated proapoptotic transcriptional regulator CHOP was among the UPR markers upregulated in neurons and oligodendrocytes, but not in astrocytes, of traumatized mouse spinal cords. To directly analyze its role in SCI, WT and CHOP null mice received a moderate T9 contusive injury. Deletion of CHOP led to an overall attenuation of the UPR after contusive SCI. Furthermore, analyses of hindlimb locomotion demonstrated a significant functional recovery that correlated with an increase in white-matter sparing, transcript levels of myelin basic protein, and Claudin 11 and decreased oligodendrocyte apoptosis in CHOP null mice in contrast to WT animals. Thus, our study provides evidence that the UPR contributes to oligodendrocyte loss after traumatic SCI.

Keywords

contusion; ER-stress; locomoter activity; oligodendrocyte; spinal cord injury; white-matter sparing

---

*Correspondence to: Scott R. Whittemore, Kentucky Spinal Cord Injury Research Center, University of Louisville School of Medicine, 511 S. Floyd St., MDR 616, Louisville, KY 40292, USA. swhittemore@louisville.edu.
Yongmei Zhao is currently at "Key Laboratory for Neurodegenerative, Diseases of Ministry of Education," Xuanwu Hospital, Capital Medical University, 45 Changchun Street, Beijing 100053, China

INTRODUCTION

Spinal cord injury (SCI) represents a severe health problem worldwide and causes life-long disability for the patients. Major hallmarks of SCI include inflammation, hypoxia, excitotoxicity, disruption of blood brain barrier, ischemia, and demyelination (Hagg and Oudega, 2006; Rowland et al., 2008). Functional loss after SCI is caused, in part, by demyelination of axons that survive the trauma (Cao et al., 2010). Understanding the key mechanisms underlying demyelination would be critical for improving functional deficits after SCI. The activation of unfolded protein response (UPR) due to endoplasmic reticulum (ER) stress is implicated in the pathogenesis of numerous CNS myelin disorders including Pelizaeus–Merzbacher disease (Southwood et al., 2002), multiple sclerosis (Lin et al., 2007), and Charcot–Marie–Tooth Neuropathy (Pennuto et al., 2008). UPR-modulated inflammation is implicated in oligodendrocyte remyelination and death in EAE (Lin et al., 2005, 2007) and cuprizone-mediated demyelination models (Lin et al., 2006). The functional role of the UPR in the pathophysiology of SCI is presently unknown.

The ER is the intracellular organelle responsible for the synthesis and proper folding of proteins to maintain cellular homeostasis. Insults that disrupt ER function induce ER stress activating the three principal UPR pathways (Ron and Walter, 2007; Schroder, 2008). ER-stress-activated protein kinase RNA (PKR)-like kinase (PERK) phosphorylates the α-subunit of elongation initiation factor 2α (eIF2α) inhibiting general translation but increasing translation of the transcription factor, activating transcription factor 4 (ATF4). Upon ER stress, inositol-requiring protein-1 (IRE-1α) executes alternative splicing of mRNA encoding the X-box-binding protein 1 (XBP1) (Yoshida et al., 2001). Finally, ER stress triggers the proteolytic processing of activating transcription factor-6 (ATF6) (Haze et al., 1999). All three pathways execute the ER stress response/UPR by regulating gene expression. The primary role of UPR is to restore ER function. However, if overstressed, the failed recovery from ER stress turns on the UPR-activated cell death. Indeed, the contribution of UPR-activated cell death has been reported in ischemic stroke (Lange et al., 2008), multiple sclerosis (Lin et al., 2006), and Alzheimer's disease (Milhavet et al., 2002). One of the components of ER stress-mediated apoptotic pathway is the transcription factor, C/EBP (CCAAT enhancer binding protein) homologous protein (CHOP). Under normal physiological conditions, CHOP is ubiquitously expressed at very low levels. However, UPR activation robustly upregulates CHOP expression in a wide variety of cells (Ron and Habener, 1992).

One initial study demonstrated UPR activation in rats after SCI (Penas et al., 2007), but its direct functional role in the mechanistic pathophysiology of traumatic SCI was not addressed. In the present study, we characterized the UPR in a mouse model of traumatic SCI and used CHOP-null mice to delineate the role of UPR-associated cytotoxicity in SCI pathology. We demonstrate specific SCI-related activation of the UPR in neurons, oligodendrocytes and astrocytes at the injury epicenter. More specifically, deletion of CHOP resulted in significant functional recovery concomitant with increased oligodendrocyte and white-matter sparing. These data strongly suggest that oligodendrocytes are a key cytotoxic target of the ERSR in response to SCI.

MATERIALS AND METHODS

Animals

CHOP null mice, completely bred to a 100% C57Bl/6 background, were procured from Jackson laboratories (Bar Harbor, ME). Age- and weight-matched wild type (WT) C57Bl/6 female mice (6–8 weeks) were obtained from Harlan (Indianapolis, IN). All animal procedures were performed according to the guidelines of University of Louisville

Institutional Animal Care and Use Committee protocols and the National Institutes of Health.

Spinal Cord Injury

Animals were anaesthetized by an intraperitoneal injection of 0.4 mg/g body weight avertin (2,2,2-tribromoethanol in 0.02 ml of 1.25% 2-methyl-2-butanol in saline, Sigma-Aldrich, St. Louis, MO). Lacri-Lube ophthalmic ointment (Allergen, Irvine, CA) was used to prevent drying of eyes, and gentamycin (50 mg/kg; Boehringer Ingelheim, St. Joseph, MO) was subcutaneously administered to reduce infection. A laminectomy was done at T9 vertebrae and moderate contusion injuries (50 kdyn force/400–600 μm displacement) were performed using the IH impactor (Scheff et al., 2003) (Infinite Horizons, Lexington, KY) as described previously (Han et al., 2010). Experimental controls included sham animals that received laminectomy only at the T9 vertebrae.

RNA Extraction, Reverse Transcriptase PCR

Total RNA was extracted from spinal cord tissue of sham and injured, WT ($n = 4$) and CHOP null mice ($n = 4$) at the injury epicenter (3 mm), and 1 cm away from injury epicenter for rostral segments (3 mm) using Trizol (Invitrogen, Carlsbad, CA) according to the manufacturer's instructions. The RNA was quantified by UV spectroscopy, and RNA integrity was confirmed on an ethidium bromide stained formaldehyde agarose gel. cDNA was synthesized with 1 μg of total RNA using the High-Capacity cDNA Synthesis Kit (Applied Biosystems, Foster City, CA) in a 20-μl reaction volume. As controls, mixtures containing all components except the RT were prepared and treated similarly. All cDNAs and control reactions were diluted 10× with water before using as a template for quantitative real time (qRT)-PCR.

Quantitative PCR Analysis

qRT-PCR was performed using ABI 7900HT Real-time PCR instrument and reagents from Applied Biosystems (Foster City, CA). Briefly, diluted cDNAs were added to Taq-man universal PCR master mix and run in triplicate. Target and reference gene PCR amplification was performed in separate tubes with Assay on Demand™ primers as follows: XBP1 (Mm00457359_m1), GRP78 (Mm01333323_g1), CHOP (Mm01135937_g1), ATF4 (Mm00515324_m1), death receptor-5 (DR5; Mm00457866_m1), GADD34 (Mm00492555_m1), MBP (Mm00521980_m1), Claudin 11 (Mm00500915_m1), and Mtap2 (Mm00485230_m1). The RNA levels were quantified using the $\Delta\Delta$CT method. Expression values obtained from triplicate runs of each cDNA sample were normalized to triplicate value for GAPDH (reference gene) from the same cDNA preparation. Transcript levels are expressed as fold changes compared with respective levels in sham controls.

XBP1 Splicing

qRT-PCR was performed with RT^2 Real-Time SYBR Green mix (SuperArray Bioscience Corporation) using spliced XBP1 (sense, gagtccgcagcaggtg; antisense, gtgtcagagtccatggga) (Hirota et al., 2006), and GAPDH (sense, ccctcaagattgtcagcaatgc; antisense, gtcctcagtgtagcccaggat) primers. The $\Delta\Delta$CT method was used for quantification. Semiquantitative RT-PCR reaction was performed using HotStarTaq enzyme (Invitrogen) in a final volume of 50 μl containing 2 μl of cDNA and 10 pmol of XBP1 primers (sense: ggccttgtggttgagaaccaggag; antisense, gaatgcc caaaaggatatcagactc) in 1× reaction buffer. Amplification cycles were: 94°C for 2 min followed by 35 cycles at 95°C for 10 s, 68°C for 30 s, and 72°C for 30 s. The final incubation was done at 72°C for 10 min. GAPDH transcript levels were used to normalize against different amounts of input RNA. XBP1 and

GAPDH PCR products were resolved on 2.5% and 1% agarose gel electrophoresis, respectively, and detected by ethidium bromide staining.

Immunohistochemical Analyses

Mice were anesthesized and transcardially perfused with ice-cold PBS. Spinal cords were dissected fresh at different time intervals post-SCI and cryopreserved at −80°C. TBS™ was used as a mounting media, and the cords were sectioned longitudinally at 20 μm and stored at −80°C until further use. For immunostaining, spinal cord sections were postfixed with ice-cold methanol for 10 min and blocked in TBS containing 5% BSA and 0.1% Triton-X-100 for 1 h at room temperature with gentle agitation. Mouse polyclonal anti-NeuN (1:100; Chemicon, Temecula, CA), goat polyclonal anti-Olig2 (1:200; Santa Cruz, Santa Cruz, CA), and mouse monoclonal antigial fibrillary acidic protein (GFAP; 1:250; Chemicon) primary antibodies were used for neurons, oligodendrocytes, and astrocytes, respectively. The ER stress primary antibodies used were as follows: rabbit polyclonal CHOP (1:100; Sigma, Ronkonkoma, NY), rabbit polyclonal ATF4 (1:100; Abcam, Cambridge, MA), rabbit polyclonal peIF2α (1:100; Biosource, Camarillo, CA), rabbit polyclonal GRP78 (1:250; Stressgen, Ann Arbor, MI), and rabbit polyclonal GADD34 (1:100; Santa Cruz). Sections were then incubated with fluorescein (1:100; FITC) and rhodamine (1:200; TRITC) conjugated F(ab′)$_2$ secondary antibodies (Jackson ImmunoResearch, West Grove, PA) for 1 h at room temperature. Confocal images were obtained using an Eclipse 90i laser confocal microscope (Nikon, Melville, NY). Negative controls used were species specific, nonimmune IgGs, or sera.

The table below details the time points at which the ER stress markers are evaluated at RNA and protein levels.

	ER stress marker	Time point
RNA	XBP1, ATF4, GADD34, CHOP, GRP78, DR5	6, 24, and 72 h
Protein	ATF4, GRP78, CHOP	6 h (neurons) and 72 h (oligodendrocytes/OPCs)

Behavioral Assessement

Open field BMS locomoter analyses were performed before injury for each animal to determine the baseline scores and weekly following SCI for 6 weeks exactly as defined by Basso et al. (2006). All raters were trained by Dr. Basso and colleagues at the Ohio State University and were blinded to animal groups.

White-Matter Sparing

Six weeks after SCI, WT and CHOP null mice were perfused transcardially with 4% paraformaldehyde (PFA). Spinal cords were submerged in 4% PFA overnight at 4°C, cryoprotected in 30% sucrose for at least 3 days at 4°C, and sectioned serially in 20-μm coronal section on a cryostat 1-cm rostral and caudal to the injury epicenter. Sections were thaw mounted on microscope slides and stored at −80°C until further use. Eriochrome cyanine (EC) was used to stain myelin to detect the extent of spared white matter (Magnuson et al., 2005; Scheff et al., 2003). Images were obtained using a Nikon Eclipse Ti inverted microscope, and white matter was traced using Nikon Elements software. The epicenter of each injury was determined based on the section with the least amount of spared white matter. A code was used to randomize the epicenter sections, allowing for unbiased, blinded quantification. The data were normalized to spared white matter in corresponding sham sections.

In Situ Hybridization

Sham and injured WT and CHOP null mice were perfused with 4% PFA 72-h postinjury. The spinal cords at the injury epicenter ±2 mm were dissected out and stored overnight in 4% PFA at 4°C. The cords were then cryoprotected in 30% sucrose and kept for at least 3 days at 4°C. TBS was used as the mounting media, and the cords were sectioned longitudinally at 20 μm and stored at –80°C until further use. *In situ* hybridization was performed with a MBP probe as described earlier (Fu et al., 2002).

Determination of Apoptosis of Oligodendrocytes *In Vivo*

Forty-eight hours after moderate contusion injury, WT and CHOP null mice were anaesthetized and trans-cardially perfused with PBS. Spinal cords were dissected, fresh frozen, blocked, and longitudinally sectioned at 20 μm on a cryostat. Every fifth section was immunostained with cleaved caspase-3 and Olig 2 antibody as described earlier. All images were captured with a Nikon TE 300 inverted microscope equipped with a Spot CCD camera using identical exposure settings. Images were acquired with a 10× objective and stitched with Elements software during acquisition. To define the regions of interest, the images of the spinal cord sections under examination were overlaid with the images of their respective adjacent GFAP-labeled sections. The injury heterodomain was defined as the area of complete absence of GFAP from the gray matter, such that the boundaries of the gray-matter injury were used to delineate the injury region of interest (Benton et al., 2008). The injury penumbral zone was then defined by expanding the heterodomain region of interest by 500 μm in a uniform fashion both horizontally and vertically (Fassbender et al., 2011). Ratio counts (Coggeshall and Lekan, 1996) were done by a blinded scorer by quantifying colocalized Olig2+cleaved caspase 3 and Olig2 cells using Elements software. Every fifth section was stained for Olig2+cleaved caspase 3 and adjacent sections with GFAP. Cell count is expressed as percentage of colocalized cells (Olig2+cleaved caspase 3) to total Olig2 cells.

Statistical Analyses

For functional assessments after injury, a repeated measures analyses of variance (ANOVA) with fixed effects and Bonferroni *post hoc t*-test was performed to detect differences in BMS score and subscores between the sham and injury groups over the 6-week testing period. Statistical analysis of qRT-PCR data was performed using independent *t*-test for means with equal or unequal variances or repeated measures ANOVA (one-way or two-way analysis of variance) followed by *post hoc* Tukey HSD test. For all other analyses, independent *t*-test for means assuming equal variance was performed.

RESULTS

SCI Leads to the Activation of UPR-Specific Markers at the Injury Epicenter

Phosphorylation of eIF2α on serine 51 (Prostko et al., 1993), a hallmark of the UPR, results in transient attenuation of protein synthesis allowing cells the opportunity to clear the accumulation of unfolded proteins. Confocal images revealed the co-localization of p-eIF2α in neurons (Fig. 1A, upper panel) and oligodendrocytes (lower panel) specifically at the injury epicenter as early as 6-h post-SCI. The presence of p-eIF2α was also observed at 24 and 72-h postinjury in neurons and oligodendrocytes (data not shown). As the ATF6-dependent UPR signaling is associated with upregulation of the ATF6 target gene XBP1, we determined its expression by qRT-PCR. A twofold increase in the expression of XBP1 mRNA at the injury epicenter at 6 h was significantly different from the rostral segment (Fig. 1B) of the lesioned cord. Increased XBP1 mRNA expression was also observed at 24-h postinjury but it declined at 72 h. In contrast, rostrally to the injury epicenter, the XBP1

mRNA levels increased in a temporal manner and reached twofold at 72 h, suggesting a spread of the pathological process from the site of primary impact into the adjacent tissue. Finally, consistent with the activation of the IRE1α-dependent pathway of the UPR (Yoshida et al., 2001), significant upregulation of an IRE1α-spliced variant of XBP1 (XBP1s) was observed at 6, 24, and 72-h postinjury at the injury epicenter (Fig. 1C, upper panel). The presence of spliced (226 bp) and unspliced XBP1 (254 bp) transcripts at 72-h post-SCI compared with shams (laminectomy controls) was confirmed by semiquantitative PCR. Together, these data indicate that SCI leads to the rapid activation of the three signaling pathways of the UPR.

SCI Leads to Upregulation of Key ER Stress Response Genes at the Injury Epicenter

ATF4, which is paradoxically translated during the eIF2α-mediated translational block leads to transactivation of the GADD34 promoter assisting in resumption of protein synthesis and induces the transcription of CHOP/GADD153 and GRP78, which may be critical for the overall cellular response to ER stress (Harding et al., 2000; Hinnebusch, 1997). To gain insight into the complex transcriptional and translational interplay of the UPR in response to SCI, we determined the expression level of these response genes. qRT-PCR analysis showed a significant 4- and 6.5-fold induction of ATF4 (Fig. 2A, $P < 0.01$) and GADD34 (Fig. 2B, $P < 0.01$) mRNAs, respectively, at the injury epicenter 6-h postinjury in contrast to rostral segments of lesioned cord. The expression level of these genes declined at 24 h, but remained higher than rostral segments ($P < 0.01$), and returned to basal levels by 72 h. Interestingly, there was also a significant threefold upregulation of both GRP78 (Fig. 2C, $P < 0.01$) and CHOP (Fig. 2D; $P < 0.01$) mRNAs at 6-h post-SCI at the injury epicenter that remained significantly higher until at least 72 h (the latest time point examined) post-SCI. Recent studies have implicated DR5 to be a direct downstream target of CHOP (Su et al., 2008). Indeed, levels of DR5 mRNA expression (Fig. 2E, $P < 0.01$) were found to be 5-, 8-, and 11-fold higher at the injury epicenter 6, 24, and 72 h, respectively, postinjury. Interestingly, DR5 mRNA expression levels remained elevated to 7.5-fold even at 1 week after injury (data not shown).

Immunohistochemical analyses further revealed these response genes to be co-localized in both neurons and oligodendrocytes. Although the expression of ATF4, GRP78, and CHOP was distinctly seen as early as 6-h postinjury in neurons (Fig. 3A–C), their oligodendrocytic expression was predominantly observed at 72 h (Fig. 4A–C). In contrast, the noninjury controls did not show any detectable expression of these markers in either neurons or oligodendrocytes (Supp. Info. Figs. 1 and 2). Colocalization of p-eIF2α with GFAP, an astrocytic marker, was absent at 6 or 24-h post-SCI. However, expression of p-eIF2α was clearly evident in astrocytes 3 days after traumatic SCI and persisted at least until 7 days (Fig. 5A). The positive cells demonstrated morphological characteristics of reactive astrocytes including stellate processes whose number and thickness were more pronounced when compared with astrocytes in sham controls. In addition, we observed colocalization of GRP78 with astrocytes at 3 (data not shown) and 7 days post-SCI (Fig. 5B). Taken together, our results indicate that traumatic injury to spinal cord results in upregulation of various ER stress response genes in all the major CNS resident cells.

Deletion of CHOP Leads to Attenuated UPR After SCI

As the UPR-associated proapoptotic CHOP was among the SCI-induced genes in neurons and oligodendrocytes, we tested its contribution to SCI pathology. Taking advantage of the CHOP KO mice, we first investigated the status of the overall UPR response affected at the level of the effector limbs in the setting of normal CHOP knockout when compared with normal WT animals. The relative gene expression values in CHOP knockout animals normalized to normal WT animals for GRP78 (1.20 ± 0.23), GADD34 (1.28 ± 0.19), ATF4

(1.27 ± 0.19), and XBP1 (1.07 ± 0.09) indicated the overall UPR response in CHOP knockout animals to be identical as in normal animals. However, qRT-PCR analysis of traumatized spinal cords of CHOP KO animals showed a significant reduction in the expression of ATF4, XBP1, GADD34, and GRP78 mRNAs levels in CHOP KO mice at 6-h postinjury when compared with WT mice (Fig. 6A). In addition, there was a significant ~65% and ~45% reduction in the expression of DR5 at 6 and 72 h after SCI, respectively, in CHOP KO mice when compared with WT mice (Fig. 6B). These data indicated that deletion of CHOP resulted in an overall attenuation of the UPR in response to SCI.

Deletion of CHOP Results in Enhanced Functional Recovery After SCI

We next examined whether deletion of CHOP, which attenuated the UPR, could contribute to functional recovery in mice with contusive SCI. WT ($n = 4$) and CHOP KO ($n = 5$) mice received moderate contusion injuries at T9 with IH impactor and were scored weekly on the open field BMS locomoter scale (Basso et al., 2006) for 6 weeks. The CHOP KO mice recovered better, apparent as early as 7 days following SCI, and exhibited significant enhanced functional outcome starting from week 2 and continuing through week 6 (the latest time point examined). The average BMS score for WT animals was 5.00 ± 0.44 at week 2, which remained constant (4.63 ± 0.75) through week 6. CHOP KO mice showed an average BMS score of 6.30 ± 0.44 ($P < 0.05$) at week 2, which increased to 7.10 ± 0.22 ($P < 0.001$) at week 6 (Fig. 7A). The WT BMS score of four to five indicates either occasional plantar stepping or frequent consistent plantar stepping with no or some coordination and paws rotated at initial contact and lift off. In contrast, all the CHOP null mice had a BMS score of 7 and above, indicative of frequent or consistent plantar stepping, which was mostly coordinated with paws parallel at initial contact and rotated at lift off (Basso et al., 2006). In terms of functional ambulation of these animals, these differences are very significant. The differences in locomoter recovery between WT and CHOP KO mice were even more profound when analyzed by BMS subscore. The average subscore for WT and CHOP KO mice were 3.0 and 5.4 at week 2 ($P < 0.05$), and 2.0 and 7.4 at week 6 ($P < 0.001$), respectively (Fig. 7B). The entire experiment was independently repeated with WT ($n = 5$) and CHOP KO ($n = 4$) mice, and the results obtained showed identical significant improved functional recovery for CHOP KO mice at week 6 ($P < 0.05$).

CHOP Contributes to White Matter Loss

To determine the possible mechanism underlying the improved functional recovery for CHOP KO mice, the spinal cords were dissected after 6 weeks of behavioral assessment and analyzed for spared white-matter. Transverse sections of WT (Fig. 8A) and CHOP KO (Fig. 8B) mice stained with the myelin stain EC were used to quantify the percentage of spared white matter at the injury epicenter. CHOP KO mice had significantly more spared white matter, 28.09% ± 3.75% ($P < 0.05$) compared with 20.83% ± 1.41% in WT mice at the injury epicenter (Fig. 8C). The level of gray-matter loss in wild and CHOP KO mice was identical reflected by the similar post-SCI Map2a,b mRNA (neuronal marker) levels (Fig. 8D), suggesting equal injury severity. With respect to oligodendrocyte survival, qRT-PCR using RNA isolated from 6-week postlesioned spinal cord showed a significant increase in transcript levels of MBP (threefold, almost back to sham levels) and claudin 11 (fourfold, 1.7 times sham levels) mRNAs (Fig. 8E, $P < 0.05$) in CHOP null mice. In addition, we show a statistically significant loss of MBP mRNA (~35%) in WT spinal cords whereas only a 22% loss in CHOP null mice at 72-h post-SCI (Fig. 9A). Claudin 11 mRNA levels did not change in WT mice after SCI, but significantly increased 50% in CHOP null mice (Fig. 9A). Real-time PCR Ct values for MBP (WT = 2.51 ± 0.08; CHOP null = 2.69 ± 0.037) and Claudin 11 (WT = 2.33 ± 0.45; CHOP null = 2.4 ± 0.288) mRNAs in sham controls (uninjured, laminectomy only) were similar, suggesting that the basal level expression of myelin in both the genotypes is the same. Moreover, transcranial magnetic motor evoked

potential (tcMMEP) responses recorded in the gastrocnemius muscles were identical between uninjured 6-week-old WT and CHOP null mice (data not shown) further supporting that initial myelin levels were similar. Supporting these data, *in situ* hybridization of longitudinal sections of CHOP null mice across the lesion epicenter revealed increased signal for MBP mRNA in the penumbral region 72-h post-SCI (Fig. 9B). Considering the role of CHOP in apoptosis, spinal cords isolated from moderately contused WT and CHOP null mice 48-h post-SCI were quantified for Olig2 colocalized with cleaved caspase 3. Caspase-3 is considered the primary executioner caspase, because it cleaves other important proteins that are necessary to accomplish apoptosis. CHOP null animals showed a significant 24.2% ($P = 0.034$; 26.2 vs 20.2) and 27.6% ($P = 0.028$; 31.0 vs 22.4) decrease in apoptotic cells at the injury epicenter and penumbra regions, respectively, when compared with WT mice at 48-h post injury (see Fig. 10). Interestingly, there was also a significant 26.3% ($P = 0.02$) increase in proliferating OPCs in CHOP null mice when compared with WT animals based on quantification of Olig2 cells colocalized with Brdu (data not shown). Collectively, white-matter sparing, qRT-PCR, *in situ* hybridization, ratio counts of apoptotic cells, and proliferating OPCs suggested oligodendrocyte sparing and OPC proliferation as the mechanism(s) by which loss of CHOP results in increased functional recovery after SCI.

DISCUSSION

The current investigation established that traumatic injury to the spinal cord resulted in an early activation of all three UPR pathways specifically at the injury epicenter implicating a role of the UPR in the pathogenesis of SCI. Importantly, we demonstrated that modulating the UPR resulted in enhanced functional recovery with a decrease in white-matter loss after SCI suggesting oligodendrocyte sparing. Our data are consistent with earlier studies showing increased levels of processed XBP1 mRNA 3–6 h after contusive SCI in mice (Aufenberg et al., 2005) and two to threefold increase in expression of GRP78, XBP1, and CHOP in contused thoracic rat spinal cord 6–24-h post-SCI (Penas et al., 2007).

Cell-Specific Induction of the UPR

The UPR was induced in neurons, oligodendrocytes, and astrocytes after SCI. Although neuronal UPR was detected for up to 24 h, oligodendrocyte UPR lasted for at least 72 h after SCI, and the astrocytic UPR was not detected before 72-h post-SCI. Consistent with our data, increased levels of peIF2α and/or GRP78 were demonstrated in neurons following ischemic, traumatic, and/or epileptic injuries (Hayashi et al., 2003; Sokka et al., 2007). Although thoracic contusive SCI is predominantly a white-matter injury and motor neuronal loss does not correlate with functional status (Magnuson et al., 2005), ERSR-mediated propriospinal neuronal loss may play a role in functional outcome. Our data showing enhanced functional recovery in CHOP null mice concomitant with a significant increase in white-matter sparing suggested oligodendrocyte protection or OPC proliferation. In addition, increased levels of oligodendrocyte-specific MBP and claudin 11 transcripts in the CHOP null mice both at 72 h and 6 weeks post-SCI further supported oligodendrocyte sparing. Consistent with our data, the UPR has been implicated in the pathogenesis of numerous CNS myelin abnormalities. In Pelizaeus–Merzbacher X-linked recessive pediatric disorder, the severity of the disease is dependent on the activation state of the UPR (Southwood et al., 2002). Leukoencephalopathy with vanishing white-matter disease in humans results in increased expression of peIF2α and GRP78 in both oligodendrocytes and astrocytes (Kollenburg et al., 2006). Moreover, the UPR modulates inflammation-mediated oligodendrocyte remyelination and death in EAE (Lin et al., 2005, 2007) and cuprizone-mediated demyelination models (Lin et al., 2006). Yet, the involvement of other CNS-resident cells, endothelial cells or immune cells cannot be ruled out as contributing to the enhanced functional recovery in CHOP null mice. Consistent with this suggestion,

endothelial cells are exceptionally vulnerable to ER stress (Erbay et al., 2009; Gargalovic et al., 2006). Although, currently, there is no direct literature showing a link between ERSR and endothelial cell death post-SCI, apoptosis can be triggered through the ATF4-CHOP signaling pathway activating CHAC1 (cation transport regulatorlike protein 1) in HAEC cells (Mungrue et al., 2009).

The sensitivity of oligodendrocytes to ER stress may be due to their highly developed ER serving the need to secrete vast amounts of myelin. Similarly, β-cells of pancreas that secrete insulin show enhanced sensitivity to ER-stress-mediated apoptosis (Maytin and Habener, 1998). The induction of peIF2α and GRP78 in astrocytes at 3 days post-SCI, which persisted at least until 1 week, suggested that the activation of astrocytic UPR is possibly due to increased synthesis/secretion of glial scar proteins (Faulkner et al., 2004; Silver and Miller, 2004). In addition, the absence of CHOP co-localized with GFAP (data not shown) suggested that most astrocytes recover from ER-stress after SCI. Our data are consistent with the increased sensitivity of oligodendrocytes to ER stress relative to that of astrocytes. We conclude that after traumatic SCI, although the UPR is activated in all major types of CNS resident cells, the temporal activation of the UPR and the decision between survival or apoptotic signaling is cell specific. Supporting this conclusion, a recent study suggested temporal differential susceptibility of CNS cell types to ER stress after SCI in rats (Penas et al., 2007).

The Role of CHOP in Functional Recovery After SCI

CHOP null mice exhibited significant functional recovery after SCI when compared with WT animals and this correlated with greater white-matter sparing. The deletion of CHOP enabled the contused mice to recover from no coordination (BMS score < 5) to mostly coordinated, weight bearing, and plantar stepping (BMS score > 7). The 9% difference in white-matter sparing for the two-point change in BMS score is consistent with the original description of the BMS (Basso et al., 2006). This is a physiologically relevant functional change that would have important therapeutic consequences if pharmacological amelioration of CHOP function could be clinically obtained. Consistent with CHOPs role in functional recovery after SCI, ablation of CHOP completely rescued motor function and reduced active demyelination by twofold in Charcot–Marie–Tooth 1B mice (Pennuto et al., 2008).

Deletion of CHOP led to enhanced functional recovery in mice, indicating an essential role of CHOP in the pathogenesis after SCI. In addition, the observation that CHOP deletion led to an attenuation of the UPR after traumatic SCI suggested that CHOP, being a key downstream target of the PERK-ATF4 arm of the UPR signaling cascade, likely contributes to a positive feedback loop enhancing the UPR in response to neurotrauma. The underlying mechanism for such feedback is not known and currently under investigation.

Upregulation of CHOP plays an important role in ER stress-induced cell death in diabetes (Oyadomari et al., 2001), brain ischemia (Kohno et al., 1997), Parkinson's disease (Holtz et al., 2003), and Alzheimer's disease (Milhavet et al., 2002). In contrast, CHOP null mice exhibited reduced apoptosis in response to ER stress (Oyadomari et al., 2001; Zinsner et al., 1998). Our data showing a decreased number of apoptotic cells and increased white-matter sparing is consistent with the suggestion of oligodendrocyte sparing in CHOP null mice after SCI.

The downstream target genes of CHOP that contribute to its proapoptotic effects are not well characterized (Sok et al., 1999). Overexpression of CHOP downregulates Bcl-2 resulting in reduced glutathione levels and proapoptotic oxidative stress (McCullough et al., 2001). As oligodendrocytes are highly sensitive to oxidative stress, such mechanism may contribute to their demise in traumatized SCI. Supporting this, following contusive thoracic

SCI, oligodendrocytes are the predominant cell type undergoing apoptosis (Li et al., 1996; Casha et al., 2001). CHOP induces the expression of numerous proapoptotic factors (DR5, TRB3, BIM, and GADD34), which promote protein synthesis and oxidative stress in stressed cells (Ohoka et al., 2005; Puthalakath, 2007; Yamaguchi and Wang, 2004). Of note, DR5, a recently identified candidate proapoptotic target gene of CHOP (Su et al., 2008), was significantly increased post-SCI and that upregulation was attenuated in CHOP-null animals. The mechanism(s) underlying SCI-related activation of CHOP and its contribution to the white-matter loss may provide novel targets for designing putative therapeutic interventions against SCI.

Although extensive literature shows direct association of the ERSR/UPR to inflammation, there is limited evidence for direct involvement of CHOP in the initiation or sustenance of the inflammatory response (Zhang and Kaufman, 2008). However, the possibility that the downregulation of the ERSR/UPR signaling in CHOP null mice leads to decreased inflammatory response and improves functional recovery cannot be ruled out. Future studies are needed to understand the physiological significance of the various ER-stress signaling pathways in mediating inflammatory responses.

The direct triggers of the SCI-associated ER stress are not known. Both oxidative damage to proteins and ER overload by newly synthesized proteins may cause ER dysfunction and UPR activation (Harding et al., 2002; Schröder and Kaufman, 2005). Previous studies demonstrated the potential role of oxidative stress in the traumatized spinal cord (Aksenova et al., 2002), suggesting the possibility of oxidative stress indicating the ERSR during the acute tissue damage phase of the SCI. Following SCI, there is also a major tissue reorganization response including reactive astrocytosis and remyelination (Faulkner et al., 2004; Lasiene et al., 2008; McTigue et al., 1998). Therefore, UPR activation by ER overload with nascent proteins may likely occur during the healing phase of the traumatic SCI.

Our findings indicate activation of the UPR in SCI pathogenesis. Currently, there is a great interest in targeting UPR for therapeutic interventions to approach functional repair in various diseases and CNS injury. Chemical chaperones like 4-phenylbutyric acid (PBA) and taurine-conjugated ursodeoxycholic acid (TUDCA) have been successfully used to reduce ER stress and restore glucose homeostasis in a mouse model of Type 2 diabetes (Ozcan et al., 2006) and are in clinical trials for a number of diseases (www.clinicaltrials.gov). Salubrinal, which inhibits eIF2α dephosphorylation, significantly reduced kainic acid-induced ER stress and neuronal death *in vivo* and *in vitro* (Sokka et al., 2007) and ameliorated hypomyelination and oligodendrocyte loss in cultured hippocampal slices exposed to IFN-γ (Lin et al., 2008). Our findings raise an interesting possibility that functional outcomes post-SCI may be improved by the use of such small molecule modulators of the UPR. Moreover, the observation that SCI activates the UPR with a delay of few hours suggests a valid therapeutic window amenable to pharmacological intervention. Furthermore, expression patterns of UPR mediators in the ventral horn motor neurons suggest that similar therapeutic strategies may prove effective when the loss of these neurons is involved in cervical or lumbar SCI or other motor neuron diseases.

Acknowledgments

References

Aksenova M, Butterfield DA, Zhang SX, Underwood M, Geddes JW. Increased protein oxidation and decreased creatine kinase BB expression and activity after spinal cord contusion injury. J Neurotrauma. 2002; 19:491–502. [PubMed: 11990354]

Aufenberg C, Wenkel S, Mautes A, Paschen W. Spinal cord trauma activates processing of XBP1 mRNA indicative of endoplasmic reticulum dysfunction. J Neurotrauma. 2005; 22:1018–1024. [PubMed: 16156717]

Basso DM, Fisher LC, Anderson AJ, Jakeman LB, McTigue DM, Popovich PG. Basso mouse scale for locomotion detects differences in recovery after spinal cord injury in five common mouse strains. J Neurotrauma. 2006; 23:635–659. [PubMed: 16689667]

Benton RL, Maddie MA, Minnillo DR, Hagg T, Whittemore SR. *Griffonia simplicifolia* isolectin B4 identifies a specific subpopulation of angiogenic blood vessels following contusive spinal cord injury in the adult mouse. J Comp Neurol. 2008; 507:1031–1052. [PubMed: 18092342]

Cao Q, He Q, Wang Y, Cheng X, Howard RM, Zhang Y, DeVries WH, Shields CB, Magnuson DS, Xu XM, Kim DH, Whittemore SR. Transplantation of ciliary neurotrophic factor-expressing adult oligodendrocyte precursor cells promotes remyelination and functional recovery after spinal cord injury. J Neurosci. 2010; 30:2989–3001. [PubMed: 20181596]

Casha S, Yu WR, Fehlings MG. Oligodendroglial apoptosis occurs along degenerating axons and is associated with FAS, p75 expression following spinal cord injury in the rat. Neuroscience. 2001; 103:203–218. [PubMed: 11311801]

Coggeshall RE, Lekan HA. Methods for determining numbers of cells and synapses: A case for more uniform standards of review. J Comp Neurol. 1996; 364:6–15. [PubMed: 8789272]

Fassbender JM, Myers SA, Whittemore SR. Activating Notch signaling post-SCI modulates angiogenesis in penumbral vascular beds but does not improve hindlimb locomoter recovery. Exp Neurol. 2011; 227:302–313. [PubMed: 21156172]

Faulkner JR, Hermann JE, Woo MJ, Tansey KE. Reactive astrocytes protect tissue and preserve function after spinal cord injury. J Neurosci. 2004; 24:2143–2155. [PubMed: 14999065]

Fu H, Qi Y, Tan M, Cai J, Takebayashi H, Nakafuku M, Richardson W, Qiu M. Dual origin of spinal oligodendrocyte progenitors and evidence for the cooperative role of Olig2 and NKx2.2 in the control of oligodendrocyte differentiation. Development. 2002; 129:681–693. [PubMed: 11830569]

Gargalovic PS, Gharavi NM, Clark MJ, Pagnon J, Yang WP, He A, Truong A, Baruch-Oren T, Berliner JA, Kirchgessner TG, Lusis AJ. The unfolded protein response is an important regulator of inflammatory genes in endothelial cells. Arterioscler Thromb Vasc Biol. 2006; 26:2490–2496. [PubMed: 16931790]

Hagg T, Oudega M. Degenerative and spontaneous regenerative processes after spinal cord injury. J Neurotrauma. 2006; 23:264–280. [PubMed: 16629615]

Harding HP, Calfon M, Urano F, Novoa I, Ron D. Transcriptional and translational control in the mammalian unfolded protein response. Annu Rev Cell Dev Biol. 2002; 18:575–599. [PubMed: 12142265]

Harding HP, Novo II, Zhang Y, Zeng H, Wek R, Schapira M, Ron D. Regulated translation initiation controls stress-induced gene expression in mammalian cells. Mol Cell. 2000; 6:1099–1108. [PubMed: 11106749]

Hayashi T, Saito A, Okuno S, Ferrand-Drake M, Chan PH. Induction of GRP78 by ischemic preconditioning reduces endoplasmic reticulum stress and prevents delayed neuronal cell death. J Cereb Blood Flow Metab. 2003; 23:949–961. [PubMed: 12902839]

Haze K, Yoshida H, Yanagi H, Yura T, Mori K. Mammalian transcription factor ATF6 is synthesized as a transmembrane protein and activated by proteolysis in response to endoplasmic reticulum stress. Mol Biol Cell. 1999; 10:3787–3799. [PubMed: 10564271]

Holtz WA, O'Malley KL. Parkinsonian mimetics induce aspects of unfolded protein response in death of dopaminergic neurons. J Biol Chem. 2003; 23:19367–19377. [PubMed: 12598533]

Hinnebusch AG. Translational regulation of yeast GCN4. A window on factors that control initiatortrna binding to the ribosome. J Biol Chem. 1997; 272:21661–21664. [PubMed: 9268289]

Hirota M, Kitagaki M, Itagaki H, Aiba S. Quantitative measurement of spliced XBP1 mRNA as an indicator of ER stress. J Toxicol Sci. 2006; 31:149–156. [PubMed: 16772704]

Kohno K, Higuchi T, Ohta S, Kumon Y, Sakaki S. Neuroprotective nitric oxide synthase inhibitor reduces intracellular calcium accumulation following transient global ischemia in the gerbil. Neurosci Lett. 1997; 224:17–20. [PubMed: 9132680]

Kollenburg van B, Dijk van J, Garbern J, Thomas AAM, Scheper GC, Powers JM, Knaap van der MS. Glia-specific activation of all pathways of the unfolded protein response in vanishing white matter disease. J Neuropathol Exp Neurol. 2006; 65:707–715. [PubMed: 16825957]

Lange PS, Chavez JC, Pinto JT, Coppola G, Sun CW, Townes TM, Geschwind DH, Ratan RR. ATF4 is an oxidative stress-inducible, prodeath transcription factor in neurons in vitro and in vivo. J Exp Med. 2008; 205:1227–1242. [PubMed: 18458112]

Lasiene J, Shupe L, Perlmutters, Horner P. No evidence for chronic demyelination in spared axons after spinal cord injury in a mouse. J Neurosci. 2008; 28:3887–3896. [PubMed: 18400887]

Li GL, Brodin G, Farooque M, Funa K, Holtz A, Wang WL, Olsson Y. Apoptosis and expression of Bcl-2 after compression trauma to rat spinal cord. J Neuropathol Exp Neurol. 1996; 55:280–289. [PubMed: 8786386]

Lin W, Bailey SL, Ho H, Harding HP, Ron D, Miller SD, Popko B. The integrated stress response prevents demyelination by protecting oligodendrocytes against immune-mediated damage. J Clin Invest. 2007; 117:448–456. [PubMed: 17273557]

Lin W, Harding HP, Ron D, Popko B. Endoplasmic reticulum stress modulates the response of myelinating oligodendrocytes to the immune cytokine interferon-γ. J Cell Biol. 2005; 169:603–612. [PubMed: 15911877]

Lin W, Kemper A, Dupree JL, Harding HP, Ron D, Popko B. Interferon-γ inhibits central nervous system remyelination through a process modulated by endoplasmic reticulum stress. Brain. 2006; 129:1306–1318. [PubMed: 16504972]

Lin W, Kunkler PE, Harding HP, Ron D, Kraig RP, Popko B. Enhanced integrated stress response promotes myelinating oligodendrocyte survival in response to interferon-gamma. Am J Pathology. 2008; 173:1508–1517.

Magnuson DS, Lovett R, Coffee C, Gray R, Han Y, Zhang YP, Burke DA. Functional consequences of lumbar spinal cord contusion injuries in the adult rat. J Neurotrauma. 2005; 22:529–543. [PubMed: 15892599]

Maytin EV, Habener JF. Transcription factors C/EBP α, C/EBP β, and CHOP(Gadd153) expressed during the differentiation program of keratinocytes in vitro and in vivo. J Invest Dermatol. 1998; 110:238–246. [PubMed: 9506442]

McCullough KD, Martindale JL, Klotz LO, AW TY, Holbrook NJ. Gadd153 sensitizes cells to endoplasmic reticulum stress by down-regulating Bcl2 and perturbing the cellular redox state. Mol Cell Biol. 2001; 21:1249–1259. [PubMed: 11158311]

McTigue DM, Horner PJ, Stokes BT, Gage FH. Neurotrophin-3 and brain-derived neurotrophic factor induce oligodendrocyte proliferation and myelination of regenerating axons in the contused adult rat spinal cord. J Neurosci. 1998; 18:5354–5365. [PubMed: 9651218]

Milhavet O, Marindale JL, Camandola S, Chan SL, Gary DS, Cheng A, Holbrook NJ, Mattson MP. Involvement of Gadd153 in the pathogenic action of presenilin-1 mutations. J Neurochem. 2002; 83:673–681. [PubMed: 12390529]

Mungrue IN, Pagnon J, Kohannim O, Gargalovic PS, Lusis AJ. CHAC1/MGC4504 is a novel proapoptotic component of the unfolded protein response, downstream of the ATF4-ATF3-CHOP cascade. J Immunol. 2009; 182:466–476. [PubMed: 19109178]

Ohoka N, Yoshii S, Hattori Ti, Onozaki K, Hayashi H. TRB3, a novel ER stress-inducible gene, is induced via ATF4-CHOP pathway and is involved in cell death. EMBO J. 2005; 24:1243–1255. [PubMed: 15775988]

Oyadomari S, Takeda K, Takiguchi M, Gotoh T, Matsumoto M, Wada I, Akira S, Araki E, Mori M. Nitric oxide-induced apoptosis in pancreatic beta cells is mediated by the endoplasmic reticulum stress pathway. Proc Natl Acad Sci. 2001; 98:10845–10850. [PubMed: 11526215]

Ozcan U, Yilmaz E, Ozcan L, Furuhashi M, Vaillancourt E, Smith RO, Gorgun CZ, Hotamisligil GS. Chemical chaperones reduce ER stress and restore glucose homeostasis in a mouse model of type 2 diabetes. Science. 2006; 313:1137–1140. [PubMed: 16931765]

Penas C, Guzmán MS, Verdú E, Forés J, Navarro X, Casas C. Spinal cord injury induces endoplasmic reticulum stress with different cell-type dependent response. J Neurochem. 2007; 102:1242–1255. [PubMed: 17578450]

Pennuto M, Tinelli E, Malaguti M, Del Carro U, D'Antonio M, Ron D, Quattrini A, Feltri ML, Wrabetz L. Ablation of the UPR-mediator CHOP restores motor function and reduces demyelination in Charcot-Marie-Tooth 1B mice. Neuron. 2008; 57:393–405. [PubMed: 18255032]

Prostko CR, Brostrom MA, Brostrom CO. Reversible phosphorylation of eurkaryotic initiation factor 2 alpha in response to endoplasmic reticular signaling. Mol Cell Biochem. 1993; 127–128:255–265.

Puthalakath H. ER stress triggers apoptosis by activating BH3-only protein Bim. Cell. 2007; 129:1337–1349. [PubMed: 17604722]

Ron D, Habener JF. CHOP, a novel developmentally regulated nuclear protein that dimerizes with transcription factors C/EBP and LAP, functions as a dominant-negative inhibitor of gene transcription. Genes Dev. 1992; 6:439–453. [PubMed: 1547942]

Ron D, Walter P. Signal integration in the endoplasmic reticulum unfolded protein response. Nat Rev Mol Cell Biol. 2007; 8:519–529. [PubMed: 17565364]

Rowland JW, Hawryluk GW, Kwon B, Fehlings MG. Current status of acute spinal cord injury pathophysiology and emerging therapies: promise on the horizon. Neurosurg Focus. 2008; 25:E2. [PubMed: 18980476]

Scheff SW, Rabchevsky AG, Fugaccia I, Main JA, Lumpp JE Jr. Experimental modeling of spinal cord injury characterization of a force-defined injury device. J Neurotrauma. 2003; 20:179–193. [PubMed: 12675971]

Schröder M. Endoplasmic reticulum stress responses. Cell Mol Life Sci. 2008; 65:862–894. [PubMed: 18038217]

Schröder M, Kaufman RJ. The mammalian unfolded protein response. Annu Rev Biochem. 2005; 74:739–89. [PubMed: 15952902]

Silver J, Miller JH. Regeneration beyond glial scar. Nat Rev Neurosci. 2004; 5:146–156. [PubMed: 14735117]

Sok J, Wang XZ, Batchvarova N, Kuroda M, Harding H, Ron D. CHOP-dependent stress-inducible expression of a novel form of carbonic anhydrase VI. Mol Cell Biol. 1999; 19:495–504. [PubMed: 9858573]

Sokka AL, Putkonen N, Mudo G, Pryazhnikov E, Reijonen S, Khiroug L, Belluardo N, Lindholm D, Korhonen L. Endoplasmic reticulum stress inhibition protects against excitotoxic neuronal injury in the rat brain. J Neurosci. 2007; 27:901–908. [PubMed: 17251432]

Southwood CM, Garbern J, Jiang W, Gow A. The unfolded protein response modulates disease severity in Pelizaeus-Merzbacher disease. Neuron. 2002; 36:585–596. [PubMed: 12441049]

Su RY, Chi KH, Huang DY, Tai MH, Lin WW. 15-deoxy-$\Delta^{12,14}$-prostaglandin J_2 up-regulates death receptor 5 gene expression in HCT116 cells: Involvement of reactive oxygen species and C/EBP homologous transcription factor gene transcription. Mol Cancer Ther. 2008; 7:3429–3440. [PubMed: 18852146]

Yamaguchi H, Wang HG. CHOP is involved in endoplasmic reticulum stress-induced apoptosis by enhancing DR5 expression in human carcinoma cells. J Biol Chem. 2004; 279:45495–45502. [PubMed: 15322075]

Yoshida H, Matsui T, Yamamoto A, Okada T, Kazatoshi M. XBP1 mRNA is induced by ATF6 and spliced by IRE1 in response to ER stress to produce a highly active transcription factor. Cell. 2001; 107:881–891. [PubMed: 11779464]

Zhang K, Kaufman RJ. From endoplasmic-reticulum stress to the inflammatory response. Nature. 2008; 454:455–462. [PubMed: 18650916]

Zinsner H, Kuroda M, Wang X, Batchvarova N, Lightfoot RT, Remotti H, Stevene JL, Ron D. CHOP is implicated in programmed cell death in response to impaired function of the endoplasmic reticulum. Genes Dev. 1998; 12:982–995. [PubMed: 9531536]
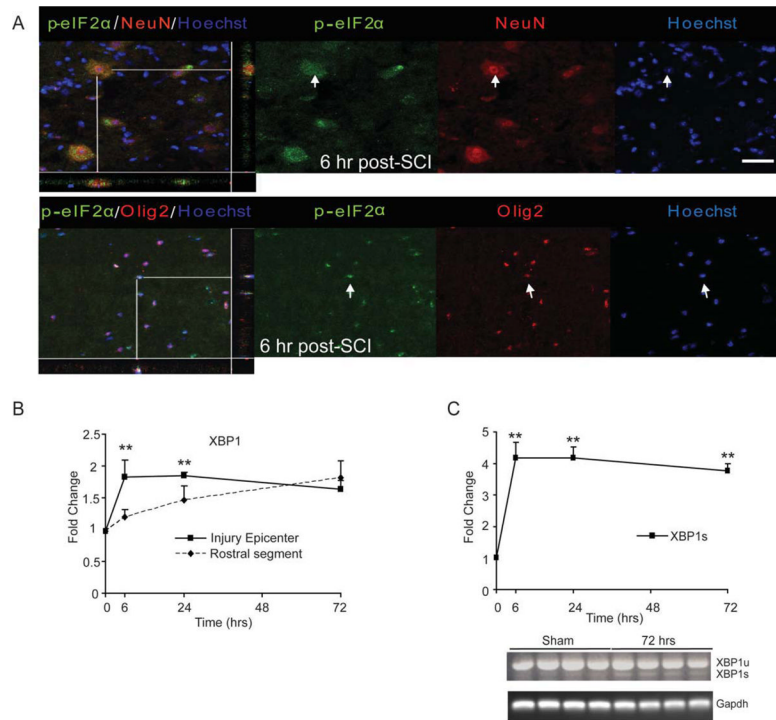
Fig. 1.
Activation of the UPR in T9 contused spinal cords of WT animals. **A:** Six hours after SCI, longitudinal sections show co-localization of p-eIF2α with neurons (upper panel) and oligodendrocytes (lower panel) at the injury epicenter. Arrows indicate the individual co-localized cells that are identified in the *XZ* and *YZ* planes in the merged images. Magnification bars = 50 μm. **B:** qRT-PCR data show levels of total XBP1 mRNA at injury epicenter and rostral segments normalized to Gapdh and expressed as fold changes compared with levels in sham controls at 6, 24, and 72-h postinjury. Increases in XBP1 mRNA levels at 6 and 24-h post-SCI indicate the activation of the ATF6 arm of the UPR. Significant difference in expression levels of XBP1 between injury epicenter and rostral segment is indicated. **C:** qRT-PCR of spliced XBP1 transcript levels (normalized to Gapdh) expressed as fold changes compared with levels in sham controls at the injury epicenter (upper panel) suggest activation of the IRE-1α arm of the UPR. Representative agarose gel shows the presence of spliced (XBP1s) and unspliced (XBP1u) transcript levels at 72-h post-SCI. Data (B, C) are the mean ± SD ($n = 4$, **$P < 0.01$).
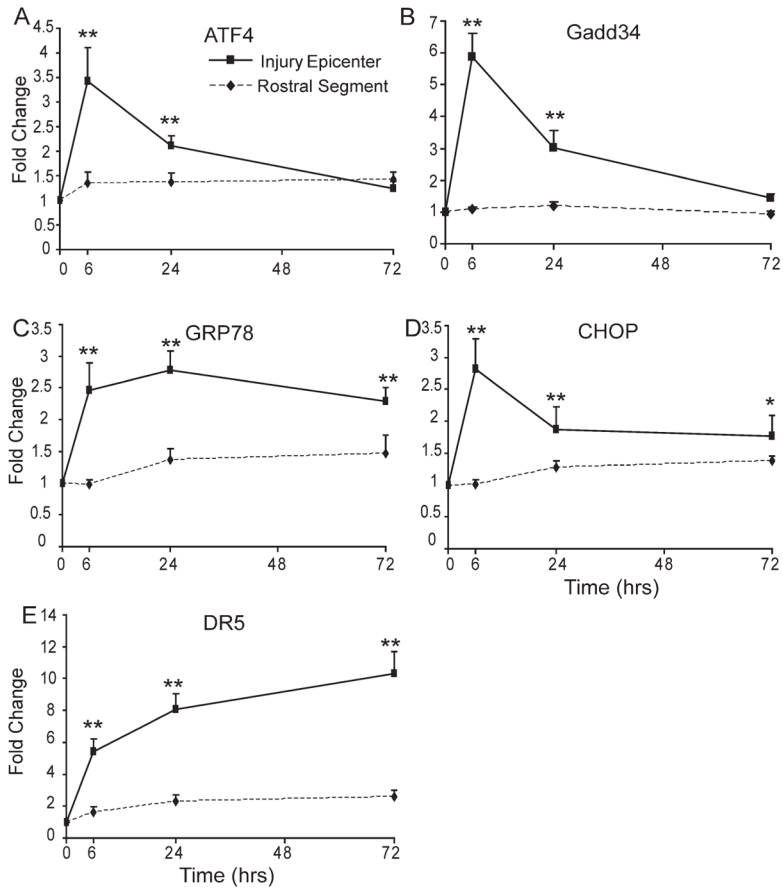
Fig. 2.
Expression of UPR mRNAs in WT animals after SCI. Transcript levels of ATF4 (**A**), GADD34 (**B**), GRP78 (**C**), CHOP (**D**), and DR5 (**E**) mRNAs were normalized to Gapdh and expressed as fold changes compared with levels in sham controls post-SCI. Significant differences in expression levels of UPR mRNAs between injury epicenter and rostral segments are indicated. Data are the mean $\pm$ SD ($n = 4$, $*P < 0.05$, $**P < 0.01$).
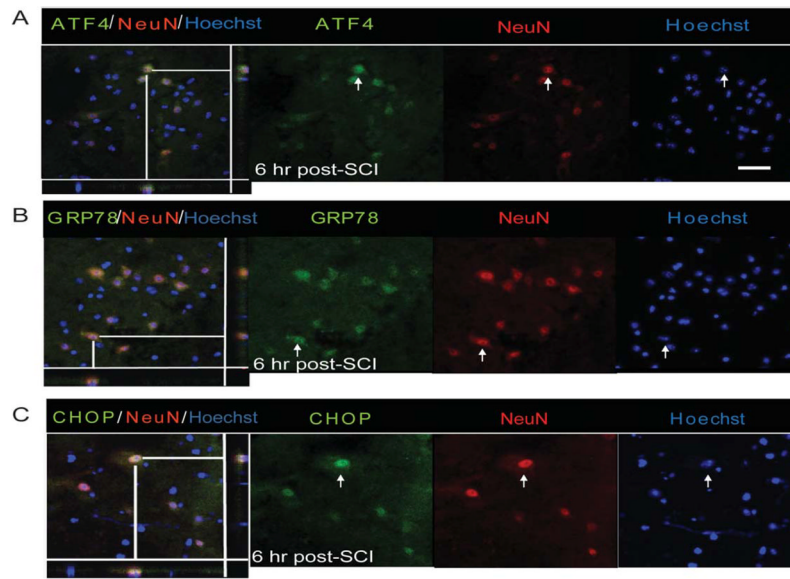
Fig. 3.
Neuronal expression of UPR markers in WT animals after SCI. Immunohistochemical analyses of longitudinal sections reveal colocalization of ATF4 (**A**), GRP78 (**B**), and CHOP (**C**) with NeuN, a neuron-specific marker, at the injury epicenter 6-h post-SCI. Arrows indicate the individual co-localized cells that are identified in the *XZ* and *YZ* planes of the merged images. Magnification bar = 50 μm. Identical data were observed in four independent experiments.
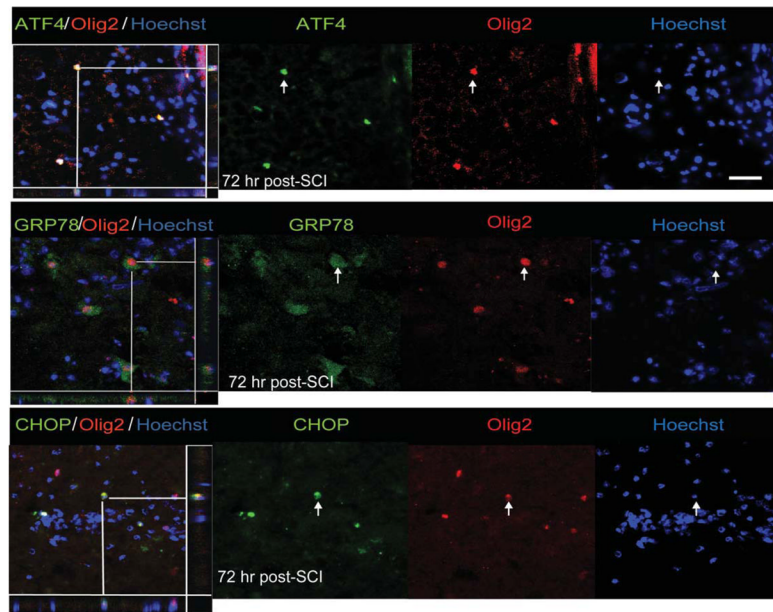
Fig. 4.
Oligodendrocyte expression of UPR markers in WT animals after SCI.
Immunohistochemical analyses of longitudinal sections reveal colocalization of ATF4 (**A**), GRP78 (**B**), and CHOP (**C**) with Olig2, an oligodendrocyte specific marker, at the injury epicenter 72-h post-SCI. Arrows indicate the individual co-localized cells one of which is identified in the *XZ* and *YZ* planes of the merged images. Magnification bar = 50 μm. Identical data were observed in four independent experiments.
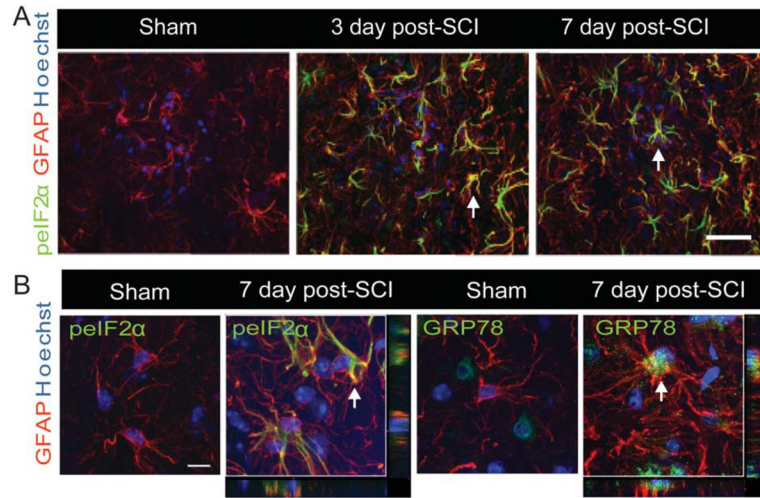
Fig. 5.
Expression of UPR markers in astrocytes of WT animals after SCI. **A:** Confocal *Z*-stacks demonstrating increased expression of peIF2α (green) with GFAP (red), an astrocyte-specific marker and Hoechst nuclear stain (blue) in sham controls and at the injury epicenter of lesioned spinal cords (3 and 7 days post-SCI). Magnification bar = 50 µm. **B:** Single confocal Z-sections taken at higher magnification show co-localization of peIF2α and GRP78 (green) with GFAP (red) at 7 days post SCI. Arrows indicate the individual co-localized cells that are identified in the *XZ* and *YZ* planes of merged images. Identical data were observed in four independent experiments.
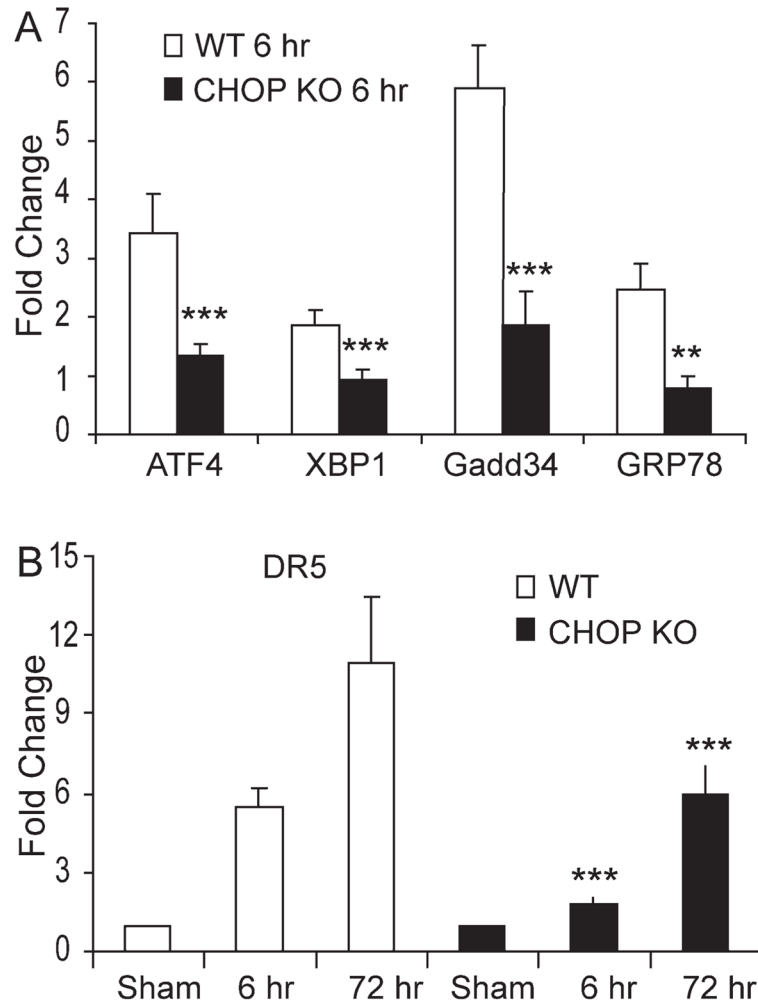
Fig. 6.
Deletion of CHOP leads to an attenuation of the UPR after SCI. **A:** Total RNA was extracted from injury epicenter of WT and CHOP KO mice 6-h post-SCI. qRT-PCR data showed significant reductions in the expression of GRP78, GADD34, ATF4, and XBP1 mRNAs in CHOP KO (black bars) mice when compared with WT (white bars) mice. **B:** DR5 mRNA levels, analyzed by qRT-PCR, were significantly reduced at the injury epicenter in CHOP KO mice (black bars) when compared with WT (white bars) mice 6 and 72-h post-SCI. DR5 mRNA levels (normalized to Gapdh) is expressed as fold changes compared with levels in sham controls. Data (A, B) are the mean $\pm$ SD ($n = 4$, $**P < 0.01$, $***P < 0.001$).
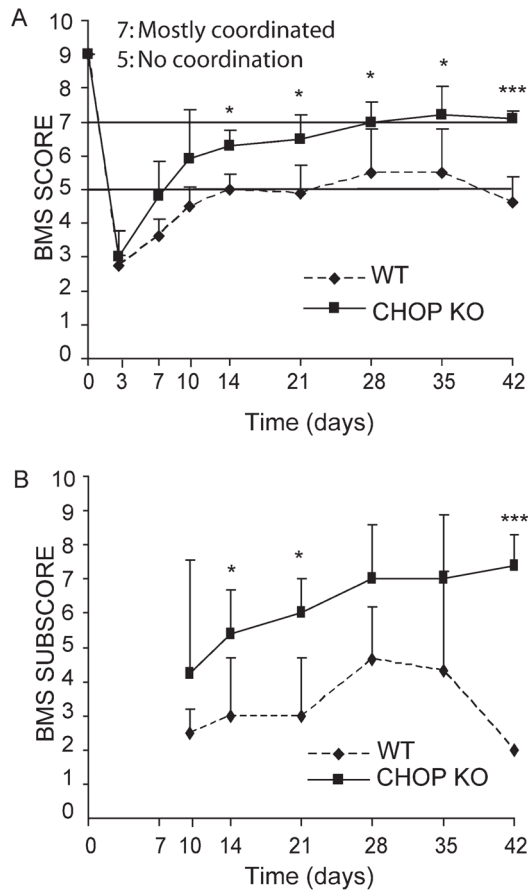
Fig. 7.
Deletion of CHOP results in enhanced functional recovery after SCI. **A:** Open field BMS locomoter analyses performed following SCI revealed a significant functional recovery in CHOP KO mice ($n = 5$; filled squares) when compared with WT ($n = 4$; filled diamonds) mice from day 14 to day 42. **B:** Analysis of BMS subscore post-SCI between WT and CHOP KO mice showed significant group differences at days 14, 21, and 42 post-SCI. Data (A, B) are the mean ± SD (*$P < 0.05$, ***$P < 0.001$; mixed-model ANOVA, *post hoc t*-test: Bonferroni). There are no subscore data at 3 and 7-day post-SCI as all BMS scores were below 5. Identical significant data were obtained in an independent replicate of this experiment ($P < 0.005$; WT; $n = 5$, CHOP null; $n = 4$).
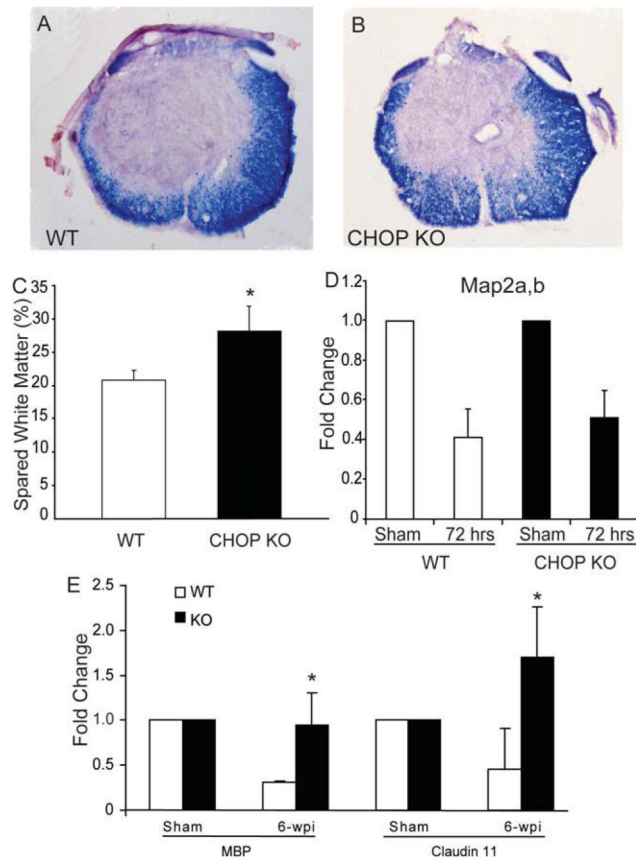
Fig. 8.
Deletion of CHOP results in increased white matter sparing. Representative histological sections from the injury epicenter stained with EC to identify myelin in (**A**) WT ($n = 4$) and (**B**) CHOP KO ($n = 5$) mice. **C:** Quantitative analysis of EC-stained sections from the injury epicenters showed a significant increase in spared white matter in CHOP KO (black bars, 28.09% ± 3.75%) when compared with WT (white bars, 20.83% ± 1.41%) mice. Data are the mean ± SD (*$P < 0.05$). **D:** qRT-PCR analysis reveal no significant differences ($P = 0.067$) in Map2a,b mRNA levels between WT (white bars) and CHOP KO (black bars) mice at 72-h postinjury, suggesting identical loss of grey matter in both groups. **E:** qRT-PCR analysis of RNA isolated from WT and CHOP null mice at 6 weeks post-SCI (6-wpi) reveal a significant increase of MBP and Claudin 11 transcript levels at the injury epicenter in CHOP null mice. Data (D, E) are the mean ± SD ($n = 4$; *$P < 0.05$).
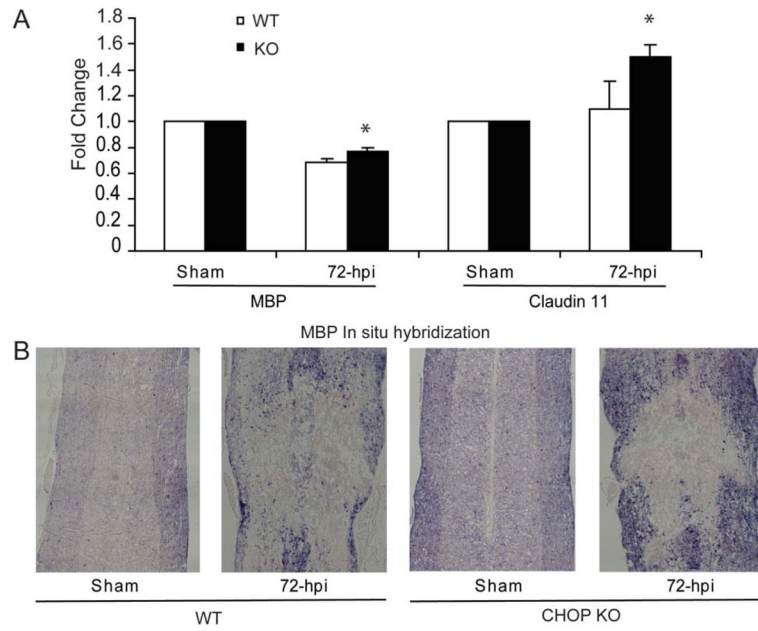
Fig. 9.
Functional recovery in CHOP null mice is partly due to oligodendrocyte sparing. **A:** Seventy-two hours post-SCI, there is a significant increase in transcript levels of MBP and Claudin 11 in CHOP null mice when compared with WT animals by qRT-PCR. Data are the mean ± SD ($n = 4$, *$P < 0.05$). **B:** *In situ* hybridization of longitudinal sections across the lesion epicenter reveals increased signal for MBP mRNA in the penumbral region of CHOP null mice 72-h post-SCI. Identical data were observed in three independent experiments.
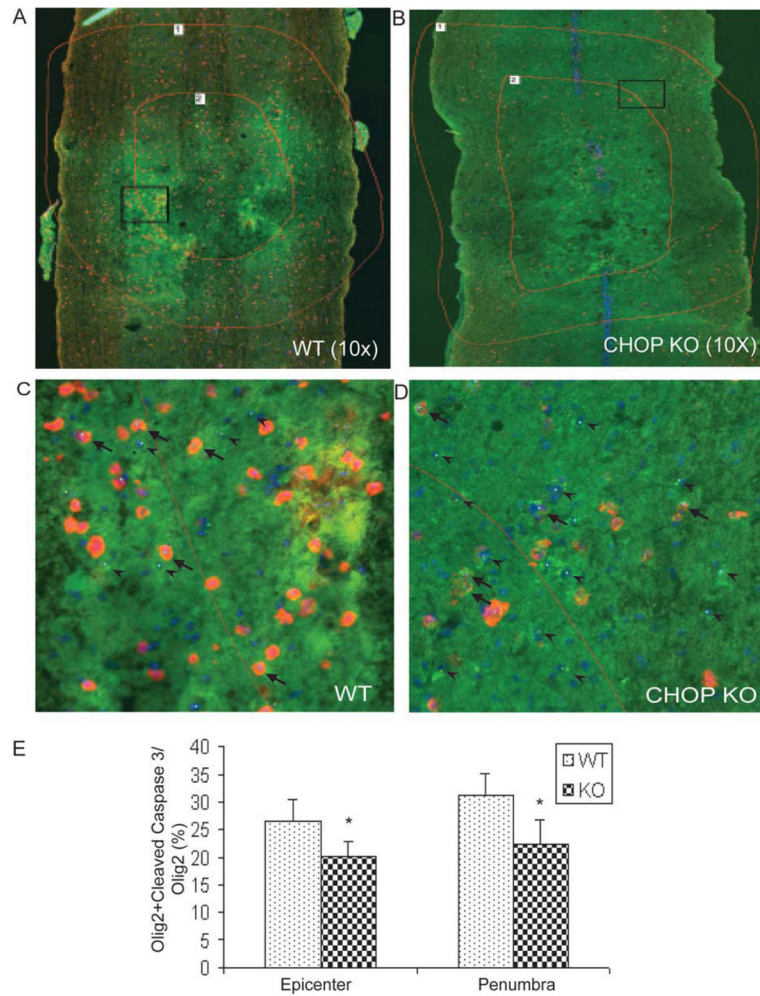
Fig. 10.
CHOP null mice exhibit less apoptotic cells after spinal cord injury. Nine 20 µm longitudinal sections (every fifth section through each cord) were immunostained and imaged under identical conditions. Representative images of (**A**) WT and (**B**) CHOP null mice ($n = 4$/group) were counted for colocalized Olig2+cleaved caspase 3 (yellow) and Olig2 (green) cells at the injury epicenter and penumbral region (shown with red lines 1 and 2). Adjacent GFAP-stained sections were used to define the injury epicenter. Zoomed images of the square boxes in A and B show the colocalized cells at higher magnification in (**C**) WT and (**D**) CHOP null mice. Arrowheads were used for Olig2 cells, and arrows were used for colocalized Olig2 + cleaved caspase 3 cells. (**E**) Quantification of Olig 2 positive cells colocalized with cleaved caspase 3 exhibited a significant 24.2% ($P = 0.034$) and 27.6% ($P = 0.028$) decrease in apoptotic cells at the injury and penumbra region, respectively, in CHOP null mice after moderate contusion injury.